International Journal of Fracture **125:** 335–348, 2004.

Time-dependent crack behavior in an integrated structure

J. LIANG[1], Z. ZHANG[*], J.H. PRÉVOST[**] and Z. SUO[*,a]
[*]*Division of Engineering and Applied Sciences, Harvard University, Cambridge, MA 02138*
[**]*Civil and Environmental Engineering Department, Princeton University, Princeton, NJ 08544*

Received 18 July 2003; accepted 7 November 2003

Abstract. Devices in modern technologies often have complex architectures, dissimilar materials, and small features. Their long-term reliability relates to inelastic, time-dependent mechanical behavior of such structures. This paper analyzes a three-layer structure consisting of, from top to bottom, an elastic film, a power-law creep underlayer, and a rigid substrate. The layers are bonded. Initially, the film is subject to a uniform biaxial tensile stress. A channel crack is introduced in the elastic film. As the underlayer creeps, the stress field in the film relaxes in the crack wake, but intensifies around the crack tip. We formulate nonlinear diffusion-like equations that evolve the displacement field. When the crack is stationary, the region in which the stress field relaxes increases with time. We identify the length scale of the region as a function of time. The stress intensity factor is proportional to the square-root of the length scale. For the power-law creep underlayer, this newly identified length depends on the film stress, and corrects an error in a previous paper by Huang, Prévost and Suo (*Acta Materialia* **50**, 4137, 2002). When the crack advances, its velocity can reach a steady state. We identify the scaling law for the steady velocity. An extended finite element method (X-FEM) is used to simultaneously evolve the creep strain and crack length. Numerical results are presented for the stress intensity factors of stationary cracks, and the steady velocities of advancing cracks.

Key words: Fracture, integrated structures, power law creep

1. Introduction

Many technologically important structures have brittle films grown on deformable materials. For instance, silica films on polymer foils serve as oxygen-barrier packaging materials in the pharmaceutical industries (Letterrier et al., 1997). Alumina scales on alloys form environmental barriers at elevated temperatures (Evans et al., 2001). Silicon nitride films are commonly used as passivation in microelectronic devices (Huang M. et al., 2002). SiGe films are wafer bonded to viscous substrates to fabricate strain-relaxed islands (Hobart et al., 2000; Yin et al., 2002). Some microelectronic applications involve thin films bonded to polymers (Martin et al., 2000; Gleskova et al., 1999). In such integrated structures, the crack behavior in the brittle films depends on the time-dependent, inelastic deformation of the materials underneath.

Figure 1 illustrates the structures to be studied in this paper. A blanket film, thickness h, lies on an underlayer, thickness H, which in turn lies on a substrate. The film is elastic, and the substrate rigid. The underlayer creeps according to the power law. The three layers are bonded. Initially, the film is in a uniform biaxial tensile stress state, σ. A channel crack is introduced into the film. If the crack is stationary, as the underlayer creeps, the stress field in the film *relaxes* in the crack wake, but *intensifies* around the crack tip. Consequently, the

[1]Present Address: Intel Corp. 2501 NW 229th Avenue Mailstop RA3-355, Hillsboro, OR 97124
[a]Corresponding author. suo@deas.harvard.edu

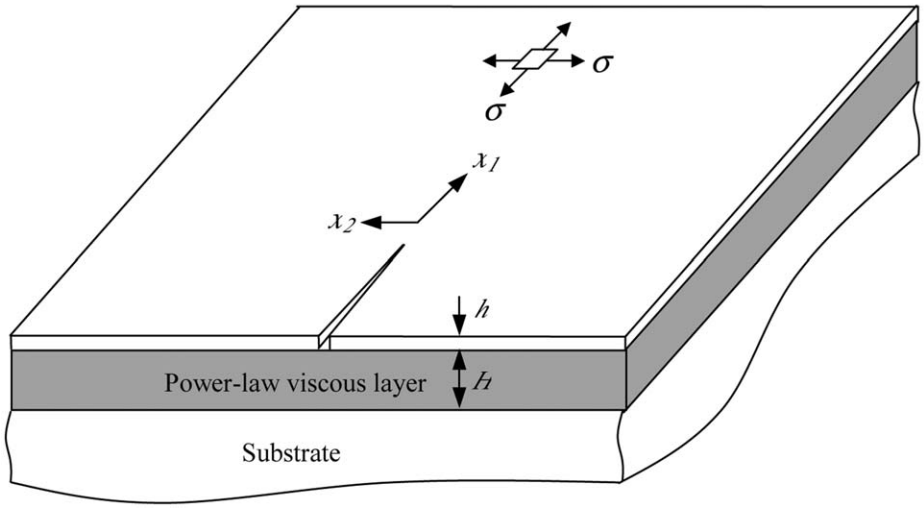

Figure 1. Schematic of the integrated structure. A brittle thin film with a pre-existing crack is bonded to a power law creeping underlayer, which in turn is bonded to a rigid substrate. The film is initially under a biaxial stress state.

crack initiates its growth after a time delay. If the crack advances slowly, the crack wake has a long time to relax, and the stress intensity at the crack tip is large. If the crack advances rapidly, the crack wake has a short time to relax, and the stress intensity at the crack tip is small. Consequently, the crack can attain a steady velocity.

In general, time-dependent crack behavior can have diverse origins. For example, when the crack velocity exceeds a fraction of the elastic wave speed, the inertia effect may be noticeable. If the crack is susceptible to subcritical growth, the crack velocity depends on the type of molecules in the environment, and how fast they reach the crack front and assist in breaking atomic bonds. If the material creeps, the crack velocity depends on the creep rate of the material. This paper highlights the underlayer creep as a cause for the time dependence, although our results are also applicable for subcritical crack growth. The effect of inertia is neglected.

Crack behavior in structures of the type illustrated in Figure 1 has been studied in the context of plate tectonics (Lehner et al., 1981) and device reliability (Xia and Hutchinson, 2000; Liang et al., 2003a; Huang R. et al., 2002; Liang et al., 2003b; Suo et al., 2003). The work done so far has focused on the linear elastic, viscous, or viscoelastic underlayer. The power-law creep underlayer, invoked in this paper, makes the problem nonlinear. We will derive the scaling laws for both stationary and advancing cracks, and use an extended finite element method to simultaneously evolve creep strains in the underlayer and the length of the crack in the film.

2. The two-dimensional shear-lag model

This section introduces the power-law creep underlayer into the model used in (Lehner et al., 1981; Xia and Hutchinson, 2000; Liang et al., 2003a; Huang R. et al., 2002; Liang et al., 2003b; Suo et al., 2003). The surface of the film coincides with the coordinate plane (x_1, x_2). Take the film under the uniform biaxial stress, σ, as the reference state, in which the displacement field vanishes. A perfect, infinite film would stay in this stress state forever. However,

if a channel crack is introduced in the film, the traction free crack faces allow the underlayer to creep. Meanwhile the film changes its stress field, starting from the crack faces, and progressively spreading over the entire film. At time t, let the in-plane displacement field be $u_\alpha(x_1, x_2, t)$, and the membrane stress field be $\sigma_{\alpha\beta}(x_1, x_2, t)$. The Greek subscript takes the values 1 and 2.

The film is elastic and isotropic. Under the plane stress conditions, Hooke's law relates the stresses to the displacement gradients:

$$\sigma_{\alpha\beta} = \sigma\delta_{\alpha\beta} + \overline{E}\left[\frac{1-\nu}{2}\left(\frac{\partial u_\alpha}{\partial x_\beta} + \frac{\partial u_\beta}{\partial x_\alpha}\right) + \nu\frac{\partial u_\gamma}{\partial x_\gamma}\delta_{\alpha\beta}\right]. \tag{1}$$

Here $\overline{E} = E/(1-\nu^2)$, E is Young's modulus, and ν is Poisson's ratio. We adopt the conventions that $\delta_{\alpha\beta} = 1$ when $\alpha = \beta$, and $\delta_{\alpha\beta} = 0$ when $\alpha \neq \beta$; and that a repeated Greek subscript implies summation over 1 and 2. The membrane stress field is the superposition of the initial stress field and that caused by the displacement gradients.

The three layers are bonded. When the elastic film slides relative to the rigid substrate, the underlayer must shear. The thickness of the underlayer is small compared to the in-plane length to be resolved, so that the shear stresses τ_α are taken to be uniform across the thickness of the underlayer. The shear strains in the underlayer, γ_α, relate to the displacements of the film as $\gamma_\alpha = u_\alpha/H$. The underlayer creeps according to the power law. Under simple shear, the shear stress, τ, relates to the shear strain-rate, $\partial\gamma/\partial t$, as $\tau = A(\partial\gamma/\partial t)^{1/n}$, where A and n are material constants. When $n = 1$, the underlayer creeps according to the linear viscous flow, and A is the viscosity. When $n \neq 1$, the creep is nonlinear. Typically, $n > 1$; thus, as the strain-rate increases, the stress increases less rapidly than that in linear viscous flow. Assuming that the material obeys the J_2 flow rule, we write for the two-dimensional shear flow

$$\tau_\alpha = \frac{A}{H^{1/n}}\left(\frac{\partial u_\beta}{\partial t}\frac{\partial u_\beta}{\partial t}\right)^{\frac{1-n}{2n}}\frac{\partial u_\alpha}{\partial t}. \tag{2}$$

The crack velocity is typically much smaller than the elastic wave speed, so that the inertia effect is negligible. The membrane stresses $\sigma_{\alpha\beta}$ act in the film, and the underlayer exerts shear stresses τ_α on the bottom face of the film. Force balance of a differential element of the film requires that

$$\frac{\partial\sigma_{\alpha\beta}}{\partial x_\beta} - \frac{\tau_\alpha}{h} = 0. \tag{3}$$

Because the film is thin, the shear stresses acting on the bottom face of the film are equivalent to body forces, $-\tau_\alpha/h$ per unit volume, distributed throughout the film. In effect, the film is in a state of plane stress subject to the body forces.

Inserting (1) and (2) into (3), we obtain the partial differential equations that evolve the displacement field $u_\alpha(x_1, x_2, t)$:

$$\overline{E}\left(\frac{1-\nu}{2}\frac{\partial^2 u_\alpha}{\partial x_\beta\partial x_\beta} + \frac{1+\nu}{2}\frac{\partial^2 u_\beta}{\partial x_\beta\partial x_\alpha}\right) = \frac{A}{hH^{1/n}}\left(\frac{\partial u_\beta}{\partial t}\right)^{\frac{1-n}{2n}}\frac{\partial u_\alpha}{\partial t}. \tag{4}$$

When $n = 1$, these equations are analogous to the classical diffusion equation. When $n \neq 1$, the diffusion-like equations are nonlinear. The traction-free condition, $\sigma_{\alpha\beta}n_\beta = 0$, holds at the crack faces, where n_β are the components of the unit vector normal to the crack faces.

Following similar arguments in (Liang et al., 2003b), despite the presence of the body force, the crack tip field takes the usual form under the plane stress conditions:

$$u_\alpha(r,\theta,t) = \frac{K(t)\sqrt{r}}{\overline{E}} U_\alpha(\theta,\nu). \tag{5}$$

The polar coordinates (r,θ) center at the crack tip. The dimensionless functions $U_\alpha(\theta,\nu)$ are given in fracture mechanics textbooks (e.g., Lawn, 1993). The stress intensity factor, $K(t)$, is time-dependent, to be determined in the following analysis.

3. Scaling law for a stationary crack

Consider a blanket film, initially under the uniform stress σ. At time $t = 0$, the presence of a stationary semi-infinite crack begins to change the stress field. Neither the traction free boundary condition, nor the initial condition, nor the governing partial differential equation (4) has any characteristic length. Consequently, we expect a self-similar solution, analogous to that of a classical diffusion equation. Let $l(t)$ be a time-dependent length; its form will be determined in the following analysis. Normalize the spatial coordinates by this length, $\hat{x}_\alpha = x_\alpha / l(t)$. A hat above a variable indicates that the variable is normalized. We guess that the displacement field takes the form

$$u_\alpha(x_1,x_2,t) = \frac{\sigma}{\overline{E}} l(t)\hat{u}_\alpha(\hat{x}_1,\hat{x}_2). \tag{6}$$

The length l absorbs the time dependence. The dimensionless functions $\hat{u}_\alpha(\hat{x}_1,\hat{x}_2)$ do not depend on time explicitly.

The time derivative of Equation (6) is

$$\frac{\partial u_\alpha}{\partial t} = \frac{\sigma}{\overline{E}} \frac{dl}{dt} \hat{f}_\alpha(\hat{x}_1,\hat{x}_2), \tag{7}$$

with $\hat{f}_\alpha(\hat{x}_1,\hat{x}_2) = (\hat{u}_\alpha - \hat{x}_\beta \partial\hat{u}_\alpha/\partial\hat{x}_\beta)$. In terms of the normalized variables, Equation (4) becomes

$$\frac{\sigma}{l}\left(\frac{1-\nu}{2}\frac{\partial^2\hat{u}_\alpha}{\partial\hat{x}_\beta\partial\hat{x}_\beta} + \frac{1+\nu}{2}\frac{\partial^2\hat{u}_\beta}{\partial\hat{x}_\beta\partial\hat{x}_\alpha}\right) = \frac{A}{hH^{1/n}}\left(\frac{\sigma}{\overline{E}}\frac{dl}{dt}\right)^{1/n}\left(\hat{f}_\gamma\hat{f}_\gamma\right)^{\frac{1-n}{2n}}\hat{f}_\alpha \tag{8}$$

Equating the coefficients on the two sides of Equation (8), we obtain that

$$l^n\frac{dl}{dt} = \overline{E}Hh^n\sigma^{n-1}A^{-n}. \tag{9}$$

This is an ordinary differential equation for the function $l(t)$. Its solution is

$$l(t) = \left[\overline{E}Hh^n\sigma^{n-1}A^{n-1}t\right]^{\frac{1}{n+1}}. \tag{10}$$

We have dropped a dimensionless factor $(n+1)$. This newly derived length corrects the erroneous Equation (19) in (Huang R. et al., 2002).

Inserting the function $l(t)$ into Equation (8), we obtain that

$$\frac{1-\nu}{2}\frac{\partial^2\hat{u}_\alpha}{\partial\hat{x}_\beta\partial\hat{x}_\beta} + \frac{1+\nu}{2}\frac{\partial^2\hat{u}_\beta}{\partial\hat{x}_\beta\partial\hat{x}_\alpha} = \left(\frac{1}{n+1}\right)^{1/n}\left(\hat{f}_\gamma\hat{f}_\gamma\right)^{\frac{1-n}{2n}}\hat{f}_\alpha. \tag{11}$$

Table 1. The calculated value κ of Equation (14). $n = 1 - 5$, $\nu = 0.3$

n	κ
1	1.0526
2	0.9109
3	0.8380
4	0.7936
5	0.7636

At time $t = 0$, $u_\alpha(x_1, x_2, 0) = 0$. In terms of the normalized variables, this initial condition becomes

$$\hat{u}_\alpha(\hat{x}_1, \hat{x}_2) \to 0, \tag{12}$$

as $(\hat{x}_1, \hat{x}_2)$ approaches infinity. The traction-free boundary condition $\sigma_{\alpha\beta} n_\beta = 0$ on the crack faces becomes

$$n_\beta \left[\frac{1-\nu}{2} \left(\frac{\partial \hat{u}_\alpha}{\partial \hat{x}_\beta} + \frac{\partial \hat{u}_\beta}{\partial \hat{x}_\alpha} \right) + \nu \frac{\partial \hat{u}_\gamma}{\partial \hat{x}_\gamma} \delta_{\alpha\beta} + \delta_{\alpha\beta} \right] = 0. \tag{13}$$

The function $\hat{u}_\alpha(\hat{x}_1, \hat{x}_2)$ is governed by the partial differential equation (11), the remote condition (12), and the boundary condition (13). Poisson's ratio ν and the power-law exponent n enter as parameters. The length l in Equation (10) absorbs the dependence on Young's modulus, film thickness, underlayer thickness, stress, as well as time.

A comparison of Equations (5) and (6) gives the scaling law of the stress intensity factor, $K = \kappa\sigma\sqrt{l}$, where κ is a dimensionless number depending on n and ν. Inserting the expression for $l(t)$, we find that

$$K = \kappa(n, \nu)\sigma^{\frac{3n+1}{2(n+1)}} \left(\overline{E} H h^n A^{-n} t \right)^{\frac{1}{2(n+1)}}. \tag{14}$$

When $n = 1$, this result reproduces that in (Huang R. et al., 2002), and the stress intensity is linear in the film stress. When $n \neq 1$, Equation (14) corrects the erroneous Equation (20) in (Huang R. et al., 2002), and the stress intensity factor is no longer linear in the film stress. Table 1 lists the numerical values of κ, which are calculated using the X-FEM, as described in Section 5.

Equation (14) gives $K = 0$ when $t = 0$, when the underlayer has not crept. This is because our model neglects the initial crack opening due to elastic deformation of the structure. Equation (14) predicts $K \to \infty$ as $t \to \infty$. This is because the crack is taken to be semi-infinite, and the film infinite. The crack starts to advance when the stress intensity factor attains a threshold value, K_{th} . The crack initiation time is obtained by equating the K in Eq. (14) to K_{th}. The stress intensity factor scales with the stress and time as

$$K \sim \sigma^{\frac{3n+1}{2(n+1)}} t^{\frac{1}{2(n+1)}}. \tag{15}$$

Consequently, the time needed for the crack to initiate its growth, t_I, scales with the film stress as $t_I \sim \sigma^{-(3n+1)}$. For a representative value of the power-law exponent, $n \approx 4$, the initiation time $t_I \sim \sigma^{-13}$, which is indeed sensitive to the film stress.

One may also use Eq. (14) in determining material properties. If all other properties are characterized, the measured initiation time determines the threshold stress intensity factor of the brittle film K_{th}. Conversely, if K_{th} is known, then by measuring the initiation times for two levels of the film stress, one can extract A and n and therefore determine the creep property of the underlayer.

4. Scaling law for a crack advancing in steady-state

We next consider a crack advancing along the x_1-axis, at a steady velocity V and a steady stress intensity factor K. Introduce dimensionless coordinates that move with the crack tip:

$$\tilde{x}_1 = \frac{x_1 - Vt}{L}, \quad \tilde{x}_2 = \frac{x_2}{L}. \tag{16}$$

To describe a steady state, the length L is independent of time, and will be determined as follows. Assume that the displacement field takes the form

$$u_\alpha(x_1, x_2, t) = \frac{\sigma}{\overline{E}} L \tilde{u}_\alpha(\tilde{x}_1, \tilde{x}_2). \tag{17}$$

The coordinate $\tilde{x}_1$ absorbs the time dependence. The dimensionless functions $\tilde{u}_\alpha(\tilde{x}_1, \tilde{x}_2)$ do not depend on time explicitly.

The time derivative of Equation (17) is

$$\frac{\partial u_\alpha}{\partial t} = -\frac{\sigma}{\overline{E}} V \frac{\partial \tilde{u}_\alpha}{\partial \tilde{x}_1}, \tag{18}$$

In terms of the normalized variables, the partial differential equation (4) becomes

$$\frac{\sigma}{L}\left(\frac{1-\nu}{2}\frac{\partial^2 \tilde{u}_\alpha}{\partial \tilde{x}_\beta \partial \tilde{x}_\beta} + \frac{1+\nu}{2}\frac{\partial^2 \tilde{u}_\beta}{\partial \tilde{x}_\beta \partial \tilde{x}_\alpha}\right) = -\frac{A}{hH^{1/n}}\left(\frac{\sigma V}{\overline{E}}\right)^{1/n}\left(\frac{\partial \tilde{u}_\beta}{\partial \tilde{x}_1}\frac{\partial \tilde{u}_\beta}{\partial \tilde{x}_1}\right)^{\frac{1-n}{2n}}\frac{\partial \tilde{u}_\alpha}{\partial \tilde{x}_1}, \tag{19}$$

The field $\tilde{u}_\alpha(\tilde{x}_1, \tilde{x}_2)$ vanishes at the infinity, and satisfies the traction-free boundary condition (13) on the crack faces.

Equating the coefficients on the two sides of Equation (19), we find that

$$L = \sigma h \left(\frac{\overline{E}H}{\sigma A^n V}\right)^{1/n}. \tag{20}$$

Poisson's ratio ν and the power-law exponent n enter as parameters, and the governing equations for $\tilde{u}_\alpha(\tilde{x}_1, \tilde{x}_2)$ are free from any other parameters. The length scale L in Equation (20) absorbs the dependence on the crack velocity, Young's modulus, the film thickness, the underlayer thickness, and the film stress.

A comparison of Equations (5) and (17) gives the scaling law of the steady stress intensity factor, $K = \chi\sigma\sqrt{L}$, where χ is a dimensionless number depending on n and ν. Inserting the expression for L, we find that

$$K = \chi(n, \nu)\sigma^{\frac{3n-1}{2n}}\left(\frac{h^n \overline{E} H}{A^n V}\right)^{\frac{1}{2n}}. \tag{21}$$

Table 2. The calculated value χ of Equation (21). $n = 1 - 5$, $\nu = 0.3$

n	χ
1	0.7303
2	0.6687
3	0.6368
4	0.6132
5	0.6011

When $n = 1$, this result reproduces the one in Liang et al. (2003b), and the stress intensity factor is linear in the film stress. When $n \neq 1$, the result is new, and the stress intensity factor is nonlinear in the film stress. Table 2 lists the numerical values of χ, which are calculated using the X-FEM, as described in Section 5. When the crack advances fast, the underlayer has little time to creep, so that the crack wake opens slightly, and the stress intensity factor is small.

If the crack advances at a critical stress intensity factor specific to the film material, K_c, Equation (21) determines the crack velocity. Of course, this requires the knowledge of K_c, the creep properties of the underlayer, as well as all other parameters in Equation (21). In experiments, the film stress σ can be controlled by an external load, and the crack velocity can be measured. Qing Ma and co-workers have used such experiments to determine the value of K_c (Ma et al., 1998). It seems also possible to use such experiments to determine the underlayer creep properties.

Many brittle solids are susceptible to subcritical crack growth (Lawn, 1993). The atomic bonds do not break when the stress intensity factor is below a threshold value K_{th}, and break instantaneously when the stress intensity factor approaches a critical value K_c. When the stress intensity factor K falls in the intermediate regime, $K_{th} < K < K_c$, the atomic bonds break at a finite rate, and the crack velocity is a function of the stress intensity factor:

$$\frac{da}{dt} = F(K). \tag{22}$$

In practice, the subcritical crack growth law is measured experimentally, and is an increasing function. When the crack grows subcritically, the intersection of the two V-K curves, Equations (21) and (22), determines the stress intensity factor and the crack velocity in the steady state.

5. Numerical results obtained using the extended finite element method

The force balance equation (3), together with the traction-free boundary condition $\sigma_{\alpha\beta} n_\beta = 0$ on the crack faces, is equivalent to the statement that

$$\int \left(\sigma_{\alpha\beta} \frac{\partial \delta u_\alpha}{\partial x_\beta} + \frac{\tau_\alpha}{h} \delta u_\alpha \right) dA = 0 \tag{23}$$

holds true for any virtual displacement field δu_α. Equation (1) expresses the membrane stresses in terms of the displacements. Equation (2) expresses the shear stresses in terms of the dis-

placement-rates. Together, Equations (23), (1) and (2) form the basis for a finite element model.

Following Belytschko and co-workers (Moës et al., 1999), we implement an extended finite element method (X-FEM). This method needs a relative coarse mesh around the crack tip, and no remeshing if the crack advances. Because the creep law is nonlinear, the nodal displacements relate to the displacement-rates by a set of nonlinear algebraic equations. We use the modified Newton-Raphson method to solve the nonlinear equations. We form the Jacobian matrix at every two iterations, for every time step. Details for implementing the XFEM can be found in Sukumar and Prévost (2003). In all calculations, Poisson's ratio is set to $\nu = 0.3$.

5.1. Shear stresses at the film/underlayer interface

As the underlayer creeps, the membrane stress field relaxes, starting from the traction-free crack faces, and progressively spreading throughout the film. At a given time t, the region in which the membrane stress field changes scales with $l(t)$ of Equation (10). To give an impression of this relaxation process, Figure 2 presents a set of contour plots of the equivalent shear stress, $\tau_e = \sqrt{\tau_1^2 + \tau_2^2}$, at the film/underlayer interface. A stationary crack, length $2a$, is in the blanket film. The underlayer creep exponent is $n = 2$. We use the dimensionless ratio l/a to indicate the time.

The shear stresses on the film/underlayer interface relate to the divergence of the membrane stresses, Equation (3). Initially, $l/a = 0$ (Figure 2a), the underlayer has no time to creep, the membrane stresses are uniform, and the shear stresses vanish. At a short time, $l/a = 2.15$ (Figure 2b), the crack opens, generating a region of high equivalent shear stress. After a long time, $l/a = 13.6$ (Figure 2c), the crack approaches the equilibrium opening, the flow of the underlayer slows down, and the equivalent shear stress around the crack decreases. Far away from the crack, the film remains undisturbed in its original equal biaxial stress state; thus, the equivalent shear stress is zero. In between these two regions, stress relaxation is still occurring appreciably; as a result, we have a region of higher equivalent shear stress. With more time (Figure 2d), this region of high equivalent shear stress travels further away from the crack.

An intriguing observation is that there are two pockets of nearly stagnant fluid ahead of the crack tip as shown in Figures 2c and 2d. The two stagnation regions occupied at symmetric positions about the crack axis. They move slowly away from the crack tip. The crack tip appears to have created a complex flow pattern that generated these two regions of relatively slow flow. Notice that the shear stresses are not singular at the crack tip. In fact, calculations show that the equivalent shear stresses are actually smaller near the crack tip than in the vicinity around the crack wake.

5.2. Semi-infinite stationary crack in a blanket film

Let t_m be an arbitrary time that ends our calculation. This time defines a length l_m according to Equation (10). To represent a blanket film, our calculation uses a $30l_m$ by $30l_m$ square film, with roller boundary conditions at the film edges. A crack of length $10l_m$ appropriately models a semi-infinite crack. The elements of size $0.02l_m$ are chosen near the crack. Larger elements are used in regions far from the crack line.

Figure 3 plots the calculated stress intensity factor as a function of time for $n = 1 - 5$. The slopes of the lines agree well with $1/[2(n + 1)]$, confirming Equation (14). Table 1 lists the

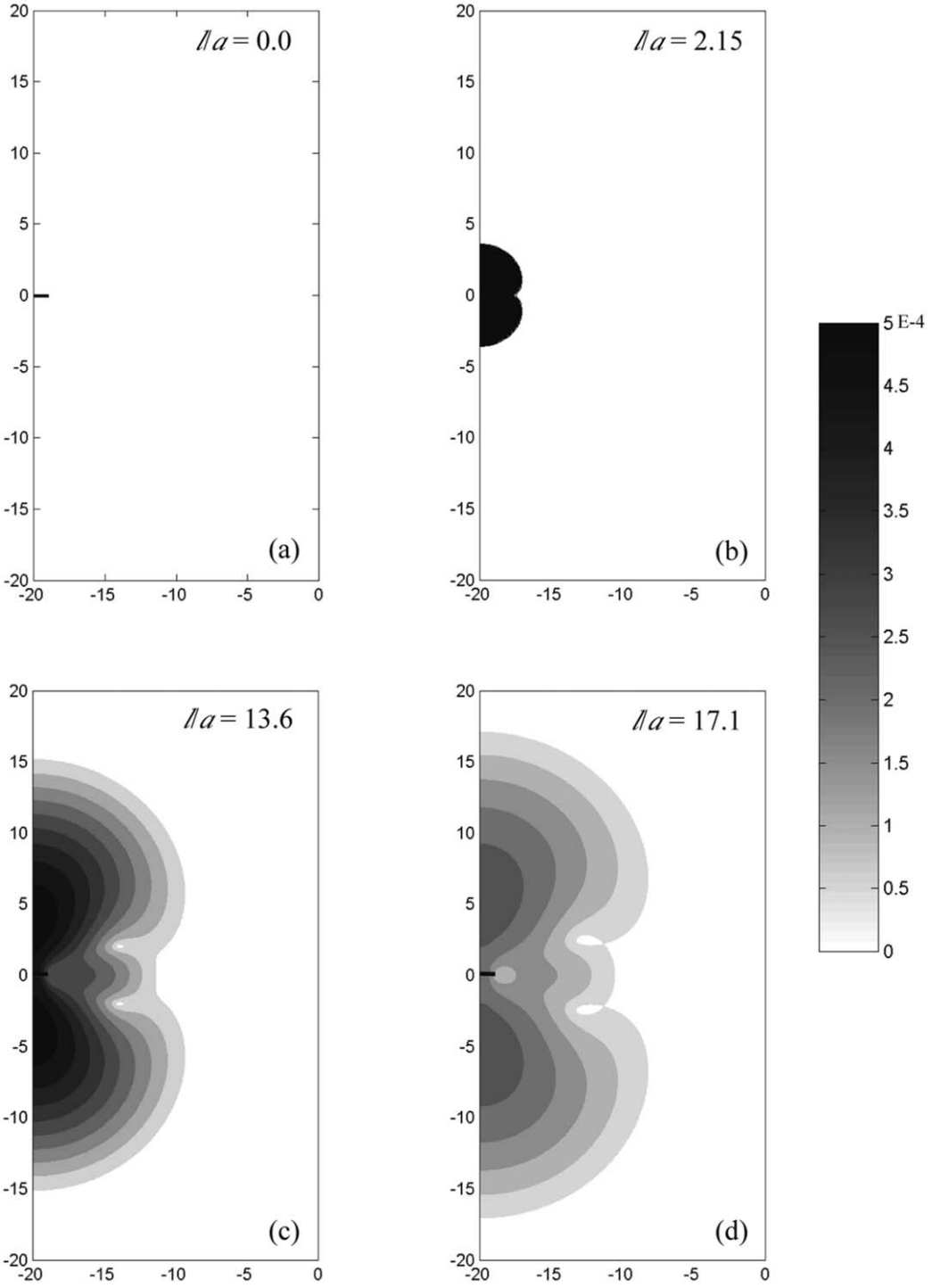

Figure 2. Contour plot of equivalent shear stress at the film/underlayer interface. The length scale is the crack size a, and the stress scale is σ.

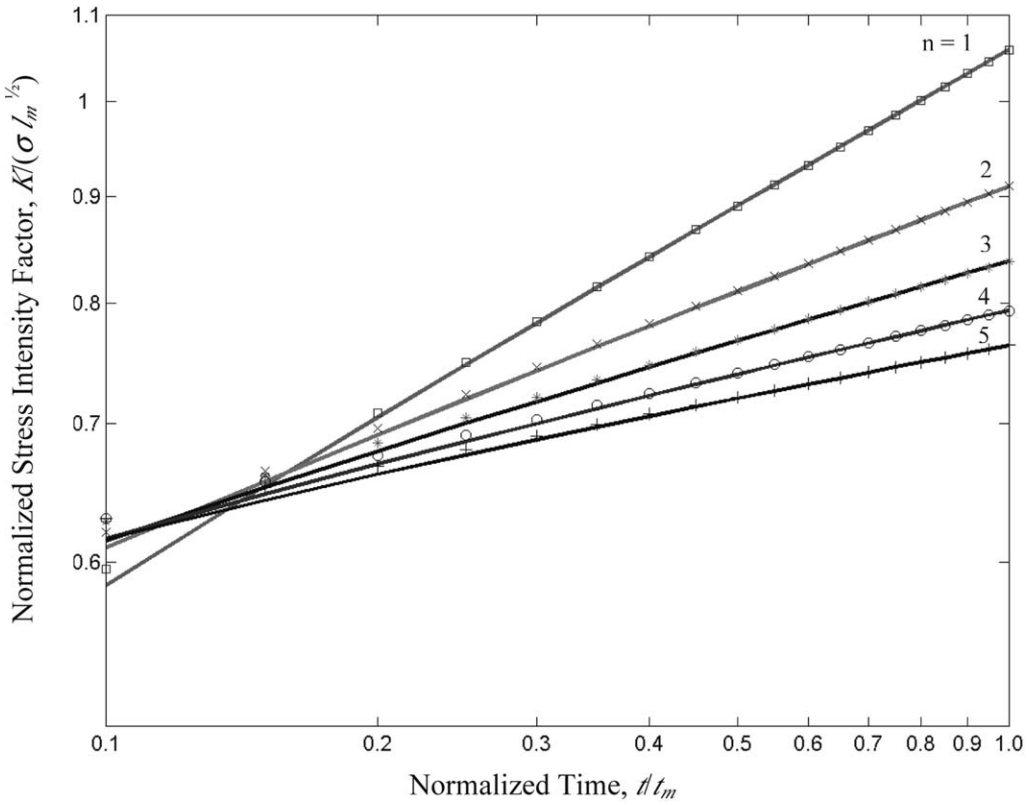

Figure 3. Normalized stress intensity factor as a function of normalized time for a semi-infinite crack in a blanket film.

calculated values of κ. For $n = 1$, the κ value obtained here compares well with the analytical value obtained by using the Laplace Transform (Suo et al., 2003).

5.3. Finite stationary crack in a blanket film

For a stationary crack, length $2a$, in a blanket film, much of Section 3 is still applicable, except that the boundary condition (13) is now applied to the finite crack, rather than the semi-infinite crack. The finite crack introduces a length, i.e., the crack length, into the problem. In the plane of the normalized coordinates $(\hat{x}_1, \hat{x}_2)$, the normalized crack length is $2a/l$. The solution $\hat{u}_\alpha(\hat{x}_1, \hat{x}_2)$ to the boundary problem will contain a/l as a dimensionless parameter, together with the creep exponent n and Poisson's ratio ν. Consequently, the stress intensity factor till takes the form $K = \kappa\sigma\sqrt{l}$, but with κ depending on a/l, n and ν. An alternative, perhaps more intuitive, scaling law is

$$K = \sigma\sqrt{\pi a}\, f\left(\frac{l}{a}, n, \nu\right). \tag{24}$$

As indicated, the dimensionless number f depends on l/a, n and ν. The time dependence is absorbed in the length l according to Equation (10). In a short time, $l/a \to 0$, the underlayer has not crept, the crack approaches a semi-infinite crack, and the stress intensity factor is given by Equation (14). In a long time, $l/a \to \infty$, the underlayer creep has affected the film over a region much larger than the crack length, so that the problem approaches that of a crack in

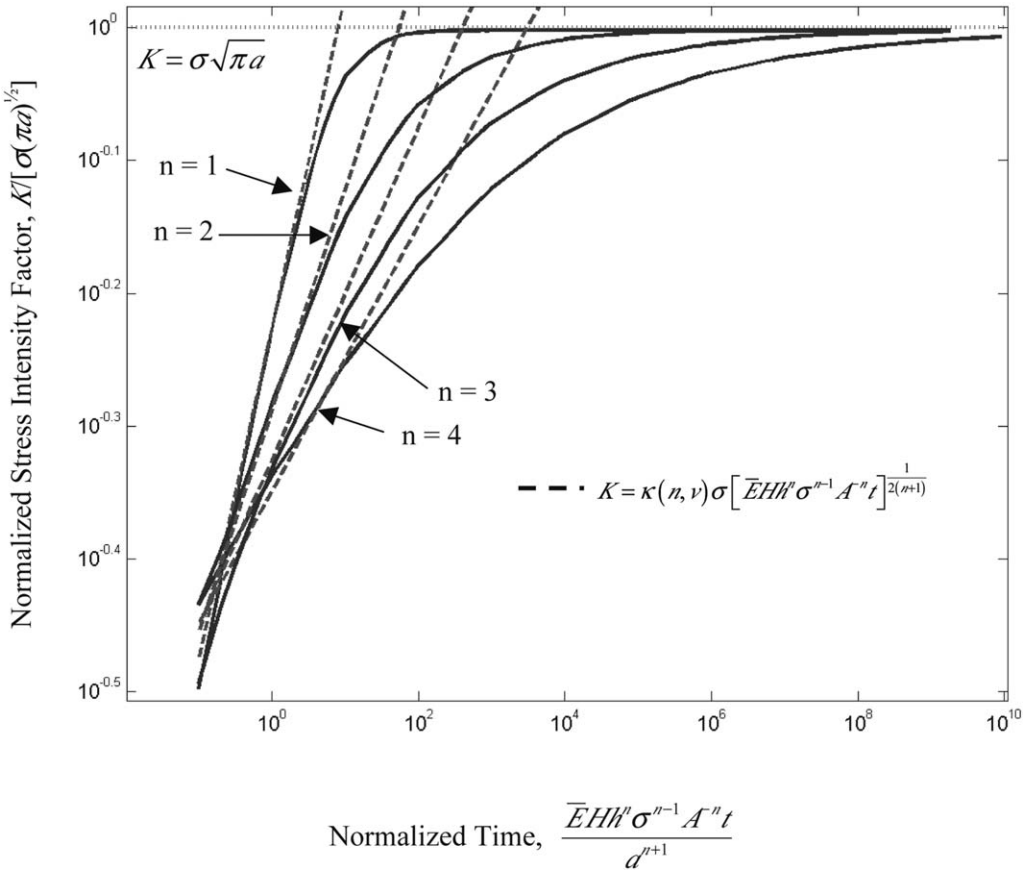

Figure 4. Normalized stress intensity factor as a function of normalized time for a finite crack in a blanket film. Also shown are the asymptotic limits.

a freestanding sheet subject to a remote stress (i.e., the Griffith crack), and the stress intensity factor approaches $K = \sigma\sqrt{\pi a}$.

Our finite element calculation uses a $20a$ by $40a$ film, with the roller boundary conditions applied on the film edges. The element size near the crack is $0.02a$ by $0.02a$. Figure 4 plots the stress intensity factor as a function of time for $n = 1 - 4$. Also shown in the figure are the two asymptotic limits for a semi-infinite crack and a Griffith crack. These results can be used to predict the time needed to initiate the growth of exiting crack. The finite crack will never grow if the threshold stress intensity factor K_{th} is above $\sigma\sqrt{\pi a}$. Otherwise, the crack will initiate its growth after a delay time.

5.4. Crack advancing in a blanket film

The scaling law for the advancing crack in the steady state, Equation (21), is independent of the detailed form of the subcritical crack growth law (22). To calculate χ using simulation, we choose to use the following simple growth law. Let K be the stress intensity factor at the crack tip, and K_0 be a parameter. The crack remains stationary if $K < K_0$, and grows when $K = K_0$. In the latter case, the crack velocity is unspecified by the subcritical crack growth law, but by the creep of the underlayer.

It is convenient to introduce a length

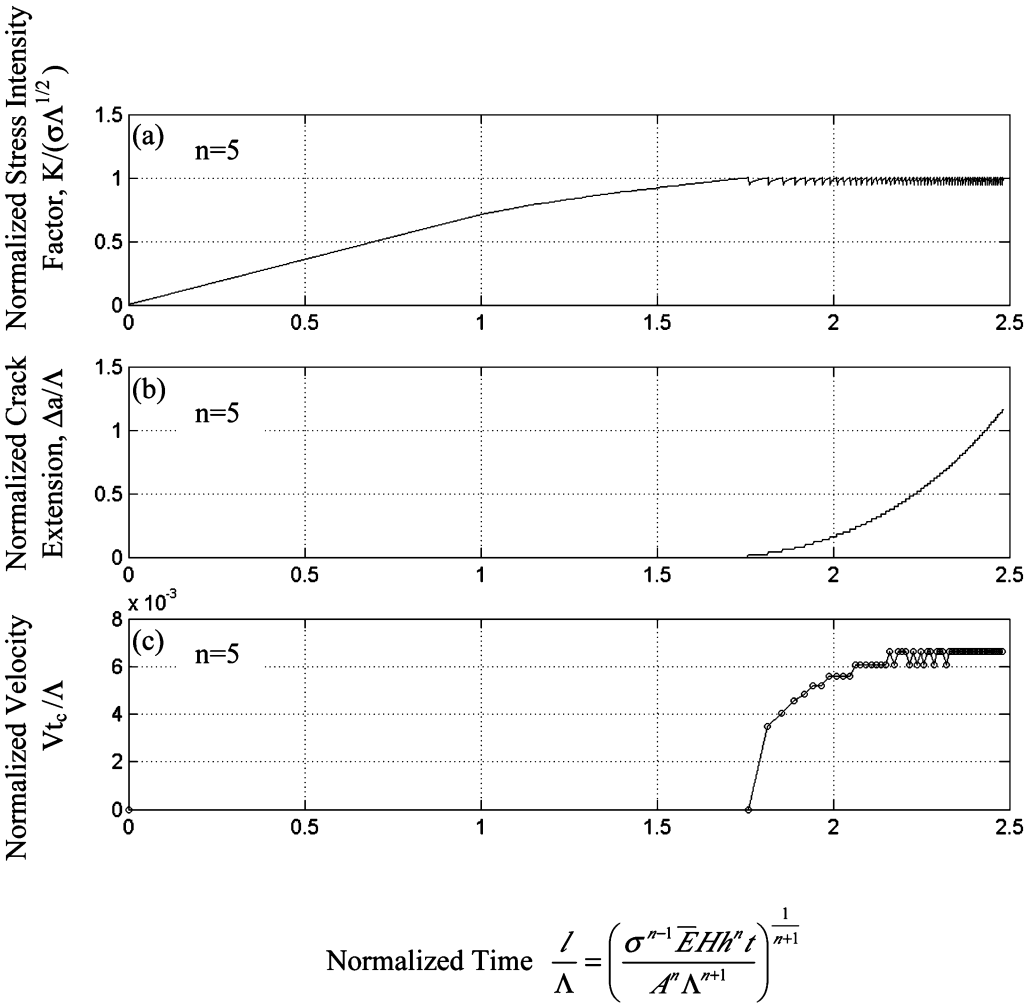

Figure 5. Time sequences for a moving crack for $n = 5$. (a) Normalized stress intensity factor. (b) Normalized crack extension. (c) Normalized crack velocity.

$$\Lambda = \left(\frac{K_0}{\sigma}\right)^2. \tag{25}$$

This length scales the distance over which the effect of the crack tip on the stress field is important. Equation (10) gives a time scale for the disturbance to propagate over this length:

$$t_c = \frac{\Lambda^{n+1}}{\bar{E} H h^n \sigma^{n-1} A^{-n}}. \tag{26}$$

Let V_0 be the steady velocity corresponding to K_0. A comparison of (21), (25) and (26) gives $V_0 = \chi^{2n}\Lambda/t_c$.

We use a 10Λ by 10Λ square film, with 0.02Λ by 0.02Λ elements near the crack and larger elements further away from the crack. The initial crack tip is positioned at the center of the film, and the roller boundary conditions are applied at the film edges. When $K < K_0$, the crack tip remains stationary, and the finite element program evolves the field and the stress intensity factor. When K reaches K_0, the program extends the crack instantaneously by an

arbitrarily specified length δa. We find $\delta a = 0.02\Lambda$ to be adequate. Because the crack has extended into a less relaxed part of the film, K drops. Further film relaxation occurs over a series of time steps while the crack remains stationary. The program calculates the time δt for K to climb back to K_0. Typically, we have 15–25 time steps in between crack extensions. The crack is allowed to extend again. This process is repeated during the calculation.

Figure 5 illustrates the computational results from a simulation done with $n = 5$. Figure 5a shows K as a function of time, increasing from zero, and then repeated dropping and arising to K_0. Figure 5b plots the crack extension as a function of time. Each time $K = K_0$, the crack length is made to advance by a prescribed amount, and the plot gives the calculated time duration for K to climb back to K_0. Figure 5c shows the crack velocity as a function of time. Initially the crack is stationary. When $K = K_0$, the crack starts to move. After a transient period, the crack attains a steady state velocity. Table 2 lists the calculated parameter χ.

6. Concluding remarks

Assuming that the underlayer creeps according to the power law, this paper extends the previous work of thin film cracking on the linear viscous or viscoelastic underlayer (Lehner et al., 1981; Xia and Hutchinson, 2000; Liang et al., 2003a; Huang R. et al., 2002; Liang et al., 2003b; Suo et al., 2003). We derive scaling laws for the stress intensity factors for stationary cracks, and steady velocities for advancing cracks. The extended finite element method is used to simulate the time-dependent crack behavior, and to calculate the coefficients in the scaling laws. At this writing, no experiments have been carried out to sort out the effects of underlayer creep and subcritical crack growth. The theoretical results in this paper provide a framework to interpret such experiments.

Acknowledgements

Our work in this area is supported by the National Science Foundation through grants CMS-9820713 and CMS-9988788 with Drs. K. Chong and J. Larsen-Basse as Program Directors.

References

Evans, A.G., Mumm, D.R., Hutchinson, J.W., Meier, G.H. and Pettit, F.S. (2001). Mechanisms controlling the durability of thermal barrier coatings. *Progress in Materials Science* **46**, 505–553.

Gleskova, H., Wagner, S. and Suo, Z. (1999). Stability of amorphous silicon transistors under extreme in-plane strain. *Applied Physics Letter* **75**, 3011–3013.

Hobart, K.D., Kub, F.J., Fatemi, M., Twigg, M.E., Thompson, P.E., Kuan, T.S. and Inoki, C.K. (2000). Compliant substrates: a comprehensive study of the relaxation mechanisms of strained films bonded to high and low viscosity oxides. *Journal of Electronic Materials* **29**, 897–900.

Huang, M., Suo, Z. and Ma, Q. (2002). Plastic ratcheting induced cracks in thin film structures. *Journal of the Mechanics and Physics of Solids* **50**, 1079–1098.

Huang, R., Prévost, J.H. and Suo, Z. (2002). Loss on constraint on fracture in thin film structures due to creep. *Acta Materialia* **50**, 4137–1448.

Lawn, B. (1993). *Fracture of Brittle Solids.* Cambridge University Press, UK.

Lehner, F.K., Li, V.C. and Rice, J.R. (1981). Stress diffusion along rupture plate boundaries. *Journal of Geophysical Research* **86**, 6155–6169.

Leterrier, Y., Boogh, L., Andersons, J. and Mansons, J.A.E. (1997). Adhesion of silicon oxide layers on poly(ethylene-terephthalate) I: effect of substrate properties on coatings fragmentation process. *Journal of Polymer Science Part B: Polymer Physics* **35**, 1449–1461.

Liang, J., Huang, R., Prévost, J.H. and Suo, Z. (2003a). Evolving crack patterns in thin films with the extended finite element method. *International Journal of Solids and Structures* **40**, 2343–2354.

Liang, J., Huang, R., Prévost, J.H. and Suo, Z. (2003b). Thin film cracking modulated by underlayer creep. *Experimental Mechanics*, in press. Preprint available at http://www.princeton.edu/ suo, Publication 132.

Ma, Q., Xie, J., Chao, S., El-Mansy, R., McFadden and Fujimoto, H. (1998). Channel cracking technique for toughness measurement of brittle dielectric thin films on silicon substrates. *Materials Research Society Symposium Proceedings* **516**, 331–336.

Martin, S.J., Godschalx, J.P., Mills, M.E., Shaffer, E.O. and Townsend, P.H. (2000). Development of a low-dielectric-constant polymer for the fabrication of integrated circuit interconnect. *Advanced Materials* **12**, 1769–1778.

Moës, N., Dolbow, J. and Belytschko, T. (1999). A finite element method for crack growth without remeshing. *International Journal of Numerical Methods in Engineering* **46**, 131–150.

Sukumar, N. and Prévost, J.H. (2003). Modeling quasi-static crack growth with extended finite element method: part I, computer implementation. *Submitted to International Journal of Solids and Structures*.

Suo, Z., Prévost, J.H. and Liang, J. (2003). Kinetics of crack initiation and growth in organic-containing integrated structures. *Submitted to Journal of the Mechanics and Physics of Solids*, Preprint available at http://www.princeton.edu/ suo, Publication 142.

Xia, Z.C. and Hutchinson, J.W. (2000). Crack patterns in thin films. *Journal of the Mechanics and Physics of Solids* **48**, 1107–1131.

Yin, H., Huang, R., Hobart, K.D., Suo, Z., Kuan, T.S., Inoki, C.K., Shieh, S.R., Duffy, T.S., Kub, F.J. and Sturm, J.C. (2002). Strain relaxation of sige islands on compliant oxide. *Journal of Applied Physics* **91**, 9716–9722.